Journal of the Korean Crystal Growth and Crystal Technology
Vol. 20, No. 3 (2010) 117-124

# Effects of impurity ($N_2$) on thermo-solutal convection during the physical vapor transport processes of mercurous chloride

Geug-Tae Kim† and Young Joo Kim*

*Department of Nano-Bio Chemical Engineering, Hannam University, Daejeon 305-811, Korea*
**Bioinformatics Research Center, Korea Research Institute of Bioscience and Biotechnology, Daejeon 305-806, Korea*

(Received April 26, 2010)
(Revised May 17, 2010)
(Accepted June 4, 2010)

**Abstract** For Ar = 5, Pr = 1.18, Le = 0.15, Pe = 2.89, Cv = 1.06, $P_B$ = 20 Torr, the effects of impurity ($N_2$) on thermally and solutally buoyancy-driven convection ($Gr_t = 3.46 \times 10^4$ and $Gr_s = 6.02 \times 10^5$, respectively) are theoretically investigated for further understanding and insight into an essence of thermo-solutal convection occurring in the vapor phase during the physical vapor transport. For $10\ K \le \Delta T \le 50\ K$, the crystal growth rates are intimately related and linearly proportional to a temperature difference between the source and crystal region which is a driving force for thermally buoyancy–driven convection. Moreover, both the dimensionless Peclet number (Pe) and dimensional maximum velocity magnitudes are directly and linearly proportional to ΔT. The growth rate is second order-exponentially decayed for $2 \le Ar \le 5$. This is related to a finding that the effects of side walls tend to stabilize the thermo-solutal convection in the growth reactor. Finally, the growth rate is found to be first order exponentially decayed for $10 \le P_B \le 200$ Torr.

**Key words** Mercurous chloride, Thermo-solutal buoyancy-driven convection, Nitrogen and physical vapor transport (PVT)

## 1. Introduction

Mercurous chloride ($Hg_2Cl_2$) materials are important for applications in acousto-optic and opto-electronic devices such as Bragg cells, X-ray detectors operating at ambient temperature [1]. The equimolar $Hg_2Cl_2$ compound decomposes to two liquids at a temperature near 525°C where the vapor pressure is above 20 atm [2, 3]. Because of this decomposition and high vapor pressure, $Hg_2Cl_2$ cannot be solidified as a single crystal directly from the stoichiometric melt. However, mercurous chloride exhibits sufficiently high vapor pressure at low temperatures so that these crystals are usually grown by the physical vapor transport (PVT) in closed silica glass ampoules. The PVT processing has many advantages over melt-growth methods since it can be conducted at low temperatures: (1) vapor-solid interfaces possess relatively high interfacial morphological stability against non-uniformities in heat and mass transfer; (2) high purity crystals are achieved; (3) materials decomposed before melting, such as $Hg_2Cl_2$ can be grown; (4) lower point defect and dislocation densities are achieved [4]. The mechanism of the PVT process is simple: sublimation-condensation in closed silica glass ampoules in temperature gradient imposed between the source material and the growing crystal. In the actual PVT system of $Hg_2Cl_2$, the molecular species $Hg_2Cl_2$ sublimes as the vapor phase from the crystalline source material ($Hg_2Cl_2$), and is subsequently transported and re-incorporated into the single crystalline phase ($Hg_2Cl_2$) [5]. Recently, PVT has become an important crystal growth process for a variety of acousto-optic materials. However, the industrial applications of the PVT process remain limited. One of important main reasons is that transport phenomena occurring in the vapor phase are complex and coupled so that it is difficult to design or control the process accurately. Such complexity and coupling are associated with the inevitable occurrence of thermal and/or solutal convection generated by the interaction of gravity with density gradients arising from temperature and/or concentration gradients. In general, convection has been regarded as detrimental and, thus, to be avoided or minimized in PVT growth system. These thermal and/or solutal convection-induced complications result in problems ranging from crystal inhomogeneity to structural imperfection. Therefore, in order to analyze and control the PVT process accurately, and also make significant improvements in the process, it is essential to investigate the roles of thermal and/or solutal convection in the PVT process.

Rosenberger's research group [6] examined the effects of thermal and thermo-solutal convections during the PVT process inside vertical cylindrical enclosures for a time-

†Corresponding author
Tel: +82-42-629-8837
Fax: +82-42-629-8835
E-mail: gtkim@hnu.kr

independent system, and showed that even in the absence of gravity, convection can be present, causing nonuniform concentration gradients. They emphasized the role of geometry in the analysis of the effects of convection. As such these fundamentally constitute steady state two-dimensional models. The steady state models are limited to low Rayleigh number applications, because the oscillation of the flow field occurs as the Rayleigh number increases. To address the issue of unsteady flows in PVT, Duval [7] performed a numerical study on transient thermal convection in the PVT processing of $Hg_2Cl_2$ very similar to the mercurous bromide for a vertical rectangular enclosure with insulated temperature boundary conditions for Rayleigh numbers up to $10^6$. Nadarajah *et al.* [8] addressed the effects of solutal convection for any significant disparity in the molecular weights of the crystal components and the inert gas. Zhou *et al.* [9] reported that the traditional approach of calculating the mass flux assuming one-dimensional flow for low vapor pressure systems is indeed correct. Rosenberger *et al.* [10] studied three-dimensional numerical modeling of the PVT yielded quantitative agreement with measured transport rates of iodine through octofluorocyclobutane ($C_4F_8$) as inert background gas in horizontal cylindrical ampoules. More recently the systematic studies on the convective effects during the physical vapor transport of mercurous chloride materials have been performed in applications of microgravity environments [11-21].

In this study, a two-dimensional model is used for the analysis of the PVT processes during vapor-growth of mercurous chloride crystals ($Hg_2Cl_2$) in horizontally oriented, cylindrical, closed ampoules in a two-zone furnace system. Diffusion-limited processes are considered in this paper, although the recent paper of Singh, Mazelsky and Glicksman [22] demonstrated that the interface kinetics plays an important role in the PVT system of $Hg_2Cl_2$. Thermally and/or solutally buoyancy-driven convection will be considered primarily for a mixture of $Hg_2Cl_2$ vapor and impurity of nitrogen ($N_2$).

It is the purpose of this paper to relate applied thermally and/or solutally buoyancy-driven (thermo-solutal) convection process parameters such as the temperature differences between the source and crystal region, aspect ratio (transport length -to-width), and the partial pressure of component B, $P_B$ (Torr) to the crystal growth rate and the maximum velocity magnitude to examine the effects of the addition of impurity ($N_2$) on thermo-solutal convection in order to gain insights into the underlying physicochemical processes.

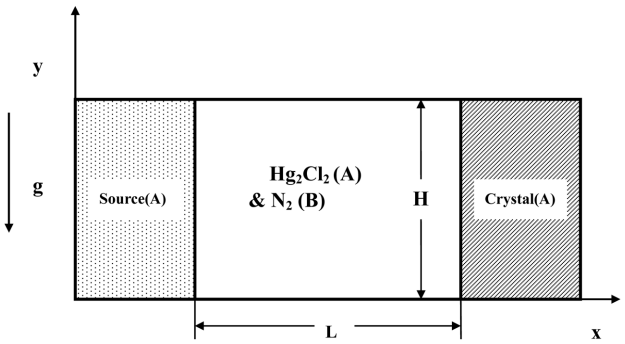


Fig. 1. Schematic of PVT growth reactor in a two-dimensional rectangular system.

## 2. Physical and Mathematical Formulations

Consider a rectangular enclosure of height H and transport length L, shown in Fig. 1. The source is maintained at a temperature $T_s$, while the growing crystal is at a temperature $T_c$, with $T_s > T_c$. PVT of the transported component A ($Hg_2Cl_2$) occurs inevitably, due to presence of impurities, with the presence of a component B ($N_2$). The interfaces are assumed to be flat for simplicity. The finite normal velocities at the interfaces can be expressed by Stefan flow deduced from the one-dimensional diffusion-limited model [23], which would provide the coupling between the fluid dynamics and species calculations. On the other hand, the tangential component of the mass average velocity of the vapor at the interfaces vanishes. Thermodynamic equilibria are assumed at the interfaces so that the mass fractions at the interfaces are kept constant at $\omega_{A,s}$ and $\omega_{A,c}$. On the vertical non-reacting walls appropriate velocity boundary conditions are no-slip, the normal concentration gradients are zero, and wall temperatures are imposed as nonlinear temperature gradients.

Thermo-physical properties of the fluid are assumed to be constant, except for the density. When the Boussinesq approximation is invoked, density is assumed constant except the buoyancy body force term. The density is assumed to be a function of both temperature and concentration. The ideal gas law and Dalton's law of partial pressures are used. Viscous energy dissipation and the Soret-Dufour (thermo-diffusion) effects can be neglected, as their contributions remain relatively insignificant for the conditions encountered in our PVT crystal growth processes. Radiative heat transfer can be neglected under our conditions, based on Kassemi and Duval [24].

The transport of fluid within a rectangular PVT crystal growth reactor is governed by a system of elliptic,

coupled conservation equations for mass (continuity), momentum, energy and species (diffusion) with their appropriate boundary conditions. Let $u_x$, $u_y$ denote the velocity components along the x- and y-coordinates in the x, y rectangular coordinate, and let T, $\omega_A$, p denote the temperature, mass fraction of species A ($Hg_2Cl_2$) and pressure, respectively.

The dimensionless variables are defined as follows:

$$x^* = \frac{x}{H},\ y^* = \frac{y}{H}, \tag{1}$$

$$u^* = \frac{u_x}{U_c},\ v^* = \frac{u_y}{U_c},\ p^* = \frac{p}{\rho_c U_c^2}, \tag{2}$$

$$T^* = \frac{T - T_c}{T_s - T_c},\ \omega_A^* = \frac{\omega_A - \omega_{A,c}}{\omega_{A,s} - \omega_{A,c}}. \tag{3}$$

The dimensionless governing equations are given by:

$$\nabla^* \bullet \vec{V}^* = 0, \tag{4}$$

$$\vec{V}^* \bullet \nabla^* \vec{V}^* = -\nabla^* p^* + Pr\nabla^{*2}\vec{V}^* - Ra \cdot Pr \cdot T^* \cdot e_g, \tag{5}$$

$$\vec{V}^* \bullet \nabla^* T^* = \nabla^{*2} T^* \tag{6}$$

$$\vec{V}^* \bullet \nabla^* \omega_A^* = \frac{1}{Le}\nabla^{*2}\omega_A^* \tag{7}$$

These nonlinear, coupled sets of equations are numerically integrated with the following boundary conditions:

On the walls ($0 < x^* < L/H$, $y^* = 0$ and 1):

$$u^*(x^*,0) = u^*(x^*,1) = v^*(x^*,0) = v^*(x^*,1) = 0 \tag{8}$$

$$\frac{\partial \omega_A^*(x^*,0)}{\partial y^*} = \frac{\partial \omega_A^*(x^*,1)}{\partial y^*} = 0,$$

$$T^*(x^*,0) = T^*(x^*,1) = \frac{T - T_c}{T_s - T_c}$$

On the source ($x^* = 0$, $0 < y^* < 1$):

$$u^*(0,y^*) = -\frac{1}{Le}\frac{\Delta\omega}{(1 - \omega_{A,s})}\frac{\partial \omega_A^*(0,y^*)}{\partial x^*}, \tag{9}$$

$$v^*(0,y^*) = 0,$$

$$T^*(0,y^*) = 1,$$

$$\omega_A^*(0,y^*) = 1.$$

On the crystal ($x^* = L/H$, $0 < y^* < 1$):

$$u^*(L/H,y^*) = -\frac{1}{Le}\frac{\Delta\omega}{(1 - \omega_{A,c})}\frac{\partial \omega_A^*(L/H,y^*)}{\partial x^*}, \tag{10}$$

$$v^*(L/H,y^*) = 0,$$

$$T^*(L/H,y^*) = 0,$$

$$\omega_A^*(L/H,y^*) = 0.$$

In the dimensionless parameters in the governing equations the thermo-physical properties of the gas mixture are estimated from gas kinetic theory using Chapman-Enskog's formulas [25].

The vapor pressure [26] $p_A$ of $Hg_2Cl_2$ (in the unit of Pascal) can be evaluated from the

$$p_A = e^{(a - b/T)}, \tag{11}$$

following formula as a function of temperature: in which a = 29.75, b = 11767.1.

The crystal growth rate $V_c$ is calculated from a mass balance at the crystal vapor interface, assuming fast kinetics, i.e. all the vapor is incorporated into the crystal, which is given by (subscripts c, v refer to crystal and vapor, respectively)

$$\int \rho_v \upsilon_v \cdot ndA = \int \rho_c \upsilon_c \cdot ndA, \tag{12}$$

$$\upsilon_c = \frac{\rho_v \int \upsilon_v \cdot ndA}{\rho_c \int dA}. \tag{13}$$

The detailed numerical schemes in order to solve the discretization equations for the system of nonlinear, coupled governing partial differential equations are found in [27].

## 3. Results and Discussion

When the molecular weight of impurity ($N_2$) is not equal to that of the crystal component ($Hg_2Cl_2$) during the physical vapor transport, both solutal and/or thermal effects should be considered. But, solutal convection would be assumed to be negligible by setting the molecular weight of component B ($N_2$) equal to that of the component A, $Hg_2Cl_2$ at density term in Eq. (5). Conductive wall boundary conditions are considered, while the insulated walls are not considered because it is difficult to obtain in practice and most of vapor growth experiments. In addition, a nonlinear thermal profile ("hump") imposed at the walls is not considered at this point which can be obtained by an often used experimental technique to prevent undesirable nucleations [28, 29]. In general, this temperature hump could eliminate the problem of vapor supersaturation along the transport path and, thus, of parasitic nucleations at the walls. But, these humps may result in sharp temperature gradients near the crystal region, inducing thermal stresses and a decrease in crystal quality.

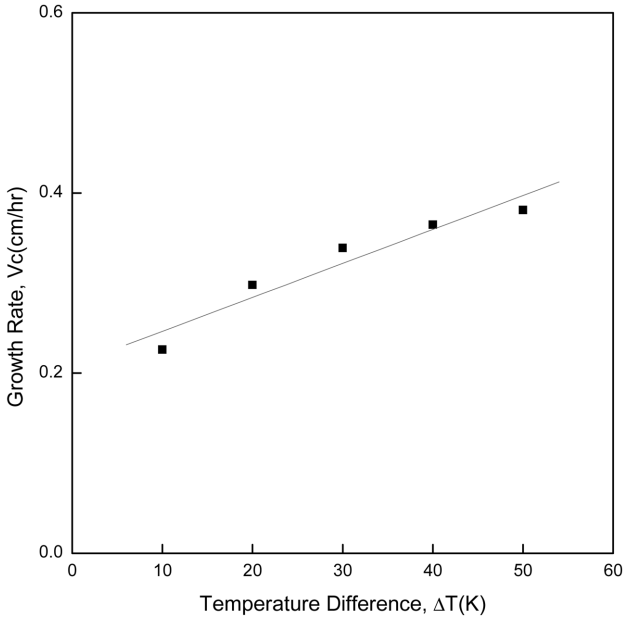


Fig. 2. Growth rates of $Hg_2Cl_2$ as a function of the temperature difference between the source and the crystal region, $\Delta T$ (K), for $10\ K \le \Delta T \le 50\ K$, Ar = 5, $P_B = 20$ Torr.

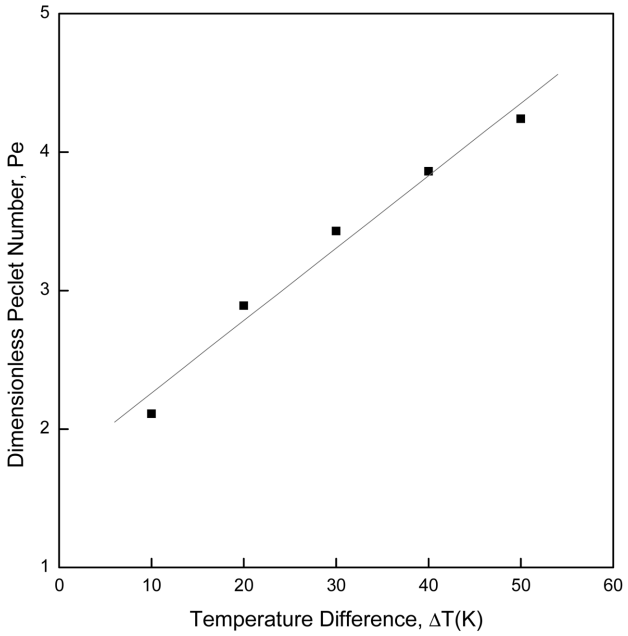


Fig. 3. Relationship between the dimensionless Peclet number, Pe and the temperature difference between the source and the crystal region, $\Delta T$ (K), corresponding to Fig. 2.

Fig. 2 shows the growth rates of $Hg_2Cl_2$ as a function of the temperature difference between the source and the crystal region, $\Delta T$ (K), for $10\ K \le \Delta T \le 50\ K$, with a linear conducting wall temperature profile. In general, with a linear temperature profile, the vapor of component A ($Hg_2Cl_2$) is in a supersaturation throughout the ampoule [16]. For $10\ K \le \Delta T \le 50\ K$, the growth rate gradually increases with the temperature difference as a slope of $2.1 \times 10^{-3}$ cm/hr•K. As not shown here, the rate increases with increasing the temperature difference, as a power law of log $\Delta T^n$ with n = 0.224. This implies that when $\Delta T$ is increased by a factor of 2, for example, form $\Delta T = 20$ K to 40 K, the corresponding rate is increased by a factor of 1.2, i.e. from 0.298 cm/hr to 0.365 cm/hr. The typical process parameters under consideration are Ar = 5, Cv = 1.06, Pr = 1.18, Le = 0.15, Pe = 2.89, $Gr_t = 3.46 \times 10^4$, $Gr_s = 6.02 \times 10^5$, based on $P_B = 20$ Torr, $T_s = 350^oC$, $\Delta T = 20$ K. The temperature difference between the source and the crystal region is a driving force for the crystal growth by the physical vapor transport. In general, the temperature difference plays a role of driving force in material processes accompanied by phase transformations, i.e., solidification, solid-liquid crystal growth, solid-vapor crystal growth etc. Fig. 3 shows a direct and linear relationship between the Peclet number, Pe and the temperature difference, $\Delta T$, corresponding to Fig. 2. Note that interfacial velocities (sublimation and condensation velocities) can be expressed in terms of a dimensionless Peclet number and a concentration parameter. The Peclet number can be also estimated by thermodynamic variables: $Pe = \ln(((P_B(L))/(P_B(0)))$ [20]. The existence of velocities at the interfaces leads to a coupling between the fluid dynamics and species calculations. Fig. 4 shows the dimensional maximum velocity magni-

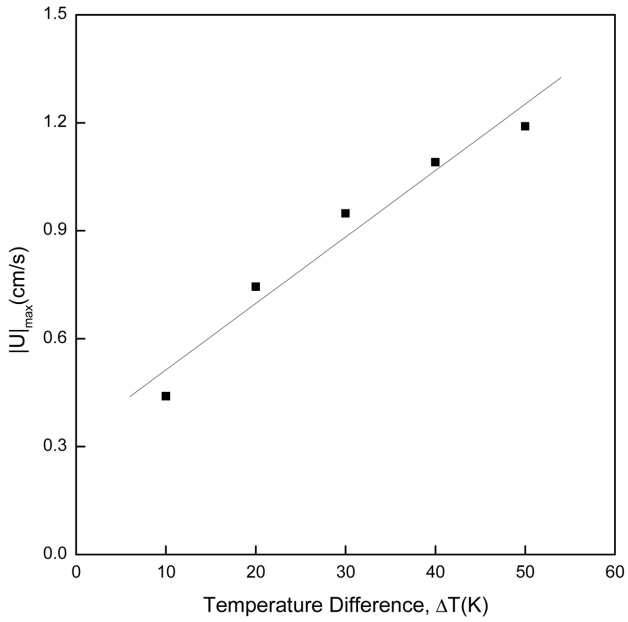


Fig. 4. The $|U|_{max}$ as a function of the temperature difference between the source and the crystal region, $\Delta T$ (K), corresponding to Fig. 2.

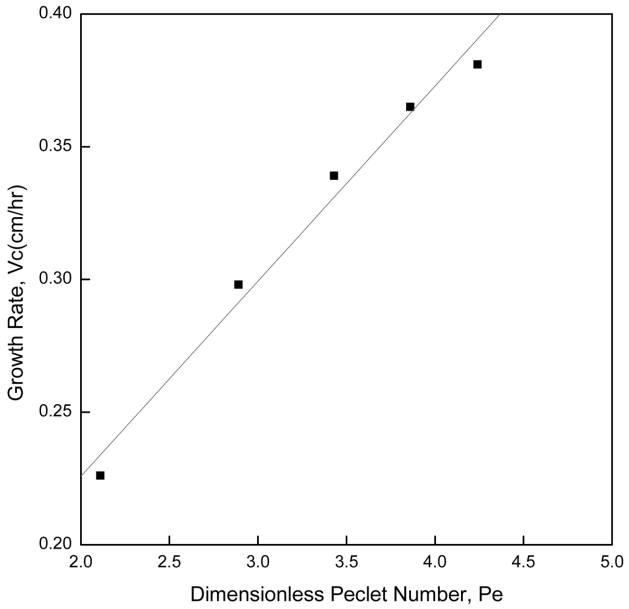


Fig. 5. Growth rates of $Hg_2Cl_2$ as a function of the dimensionless Peclet number, corresponding to Fig. 2.

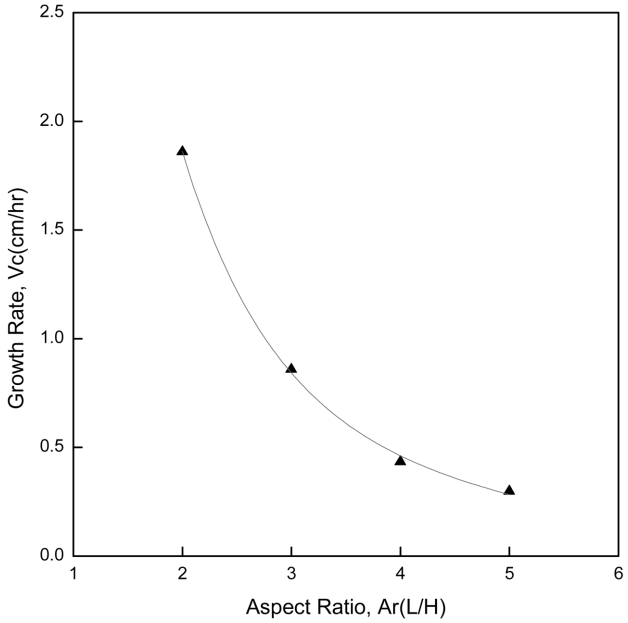


Fig. 6. Effects of aspect ratio Ar (L/H) on the crystal growth rates of $Hg_2Cl_2$, with the height, H fixed.

tude, $|U|_{max}$ is proportional to the temperature difference $\Delta T$, which corresponds to Fig. 2. Note the dimensional maximum velocity magnitude, $|U|_{max}$ implies the importance of intensity of convection during physical vapor transport. Fig. 5 shows the growth rates of $Hg_2Cl_2$ as a function of the dimensionless Peclet number, Pe, corresponding to Fig. 2. Comparison of Fig. 2 with 5 supports the effects of temperature difference on the growth rate and the Peclet number, and reflects the dependence of the growth rate on the Peclet number. Therefore, the rate and the Peclet number and $|U|_{max}$ are directly and intimately dependent on the temperature difference, which indicates thermally buoyancy-driven convection plays an important role in the vapor phase during the physical vapor transport. It should be noted that for the processes under consideration, the convective intensity caused by the solutally buoyancy-driven convection ($Gr_s = 6.02 \times 10^5$) is greater than by the thermally buoyancy-driven convection ($Gr_t = 3.46 \times 10^4$) by one order of magnitude.

Fig. 6 shows the effects of aspect ratio Ar (L/H) on the growth rates of $Hg_2Cl_2$ for $\Delta T = 50$ K, $P_B = 20$ Torr, $T_s = 350^oC$ with fixed width H. The rate is second order-exponentially decayed with the aspect ratio, Ar (L/H). This is intimately related with the effects of side walls which suppress the thermo-solutal convection flow inside the growth enclosure. It is not surprising that the effects of side walls tend to stabilize the thermo-solutal convection in the growth reactor. This tendency is consistent with the results [30] on the pure thermal convection without crystal growth in enclosures. The rate is decreased sharply for the range from $Ar = 2$ to 3 by a factor of 0.46, and then for $3 \le Ar \le 5$, is decreased by a factor of 0.35. Note the numerical executions for $1 \le Ar \le 1.7$ cannot be performed, which is likely to be chaotic flows. As shown in Fig. 7, $|U|_{max}$ has the same trend and decreasing degree as the rate against the aspect ratio. In other words, the decreasing degree is approximately

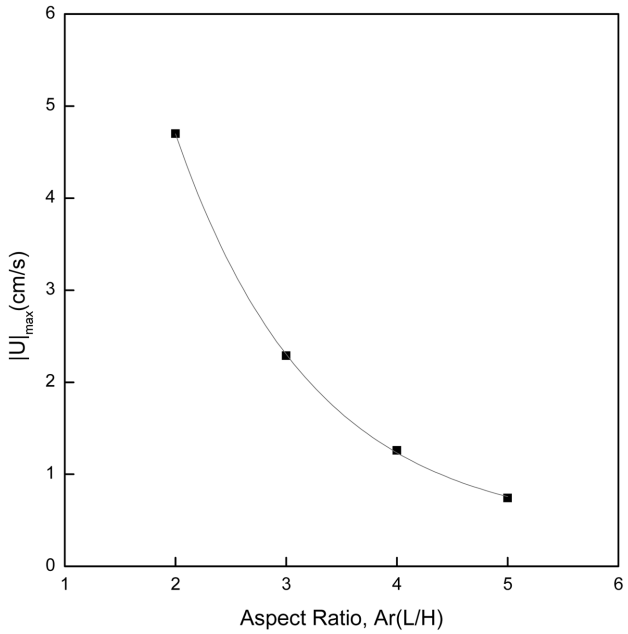


Fig. 7. The $|U|_{max}$ as a function of the aspect ratio Ar (L/H), corresponding to Fig. 6.

0.48 for $2 \le Ar \le 3$, and 0.32 for $3 \le Ar \le 5$, respectively. Note in actual crystal growth systems, the temperature profile is intimately related to the aspect ratio because the temperature profile is so imposed that it could not be altered. In this study, the conducting wall boundary conditions are used for the thermal boundary conditions at walls and the temperature profiles are linear. Figs. 6 and 7 are based on $\Delta T = 50$ K and $P_B = 20$ Torr.

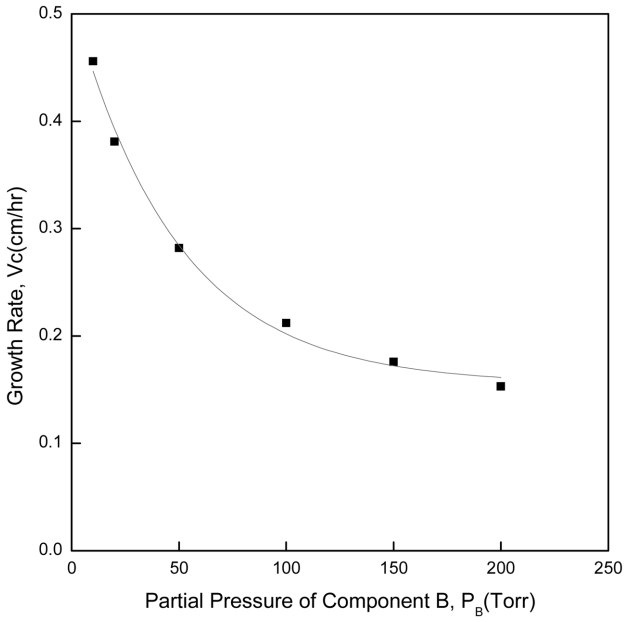


Fig. 8. Effects of partial pressure of component B, $P_B$ (Torr) on the crystal growth rates of $Hg_2Cl_2$.

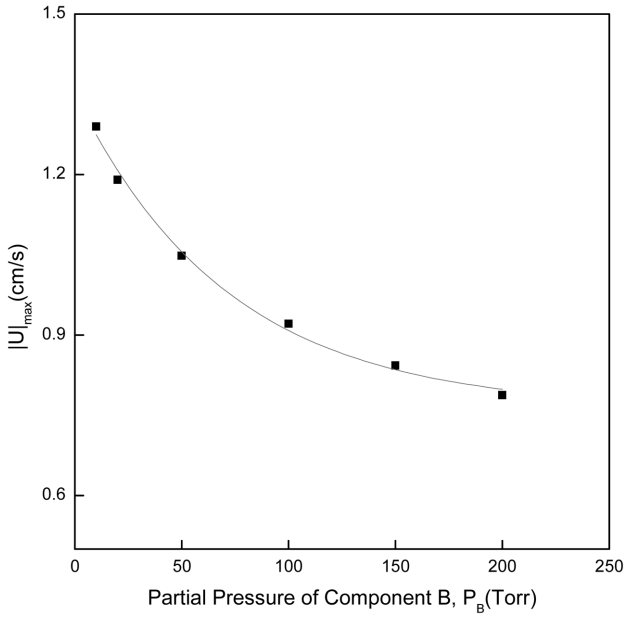


Fig. 9. The $|U|_{max}$ as a function of the aspect ratio Ar (L/H), corresponding to Fig. 8.

Fig. 8 shows the growth rates of $Hg_2Cl_2$ as a function of partial pressure of component B, $P_B$ (Torr) for $\Delta T = 50$ K, $Ar = 5$. Like the case of aspect ratio, Ar (L/H), the rate is first order-exponentially decayed with $P_B$ (Torr) for the range of 10 Torr $\le P_B \le$ 200 Torr. For 10 Torr $\le P_B \le$ 50 Torr, the rate is decreased significantly by the factor of 0.62, and for 50 Torr $\le P_B \le$ 200 Torr, reduced by a factor of 0.54. As shown in Figs. 8 and 9, $|U|_{max}$ is first order-exponentially decayed against the partial pressure of component B, $P_B$ (Torr) like the growth rate. But the decreasing degree is approximately 0.81 for 10 Torr $\le P_B \le$ 50 Torr, and 0.75 for 50 Torr $\le P_B \le$ 200 Torr, respectively. Figs. 8 and 9 are based on $\Delta T = 50$ K, $Ar = 5$, and $T_s = 350^{\circ}C$ with fixed width H. From a point of view of sensitivity of growth rate versus process parameters, comparisons of Figs. 2, 6 and 8 illustrate the partial pressure of component B the side affects more significantly on the growth rate than thermal convective effects such as the temperature difference, aspect ratio.

Figs. 10 through 12 show the interfacial distribution of growth rates along the y-direction of the crystal surface, corresponding to Fig. 2, 6, 8, respectively. As shown in Fig. 10, with increasing the temperature difference, the interfacial distribution of growth rate becomes asymmetrical against y = 1.0. The maximum growth rate occurs in the neighborhood of y = 0.5.

As the temperature difference approaches 50 K, a gap between the maximum growth rates at 40 K and 50 K in the neighborhood of y = 0.5 becomes reduced. Fig. 11

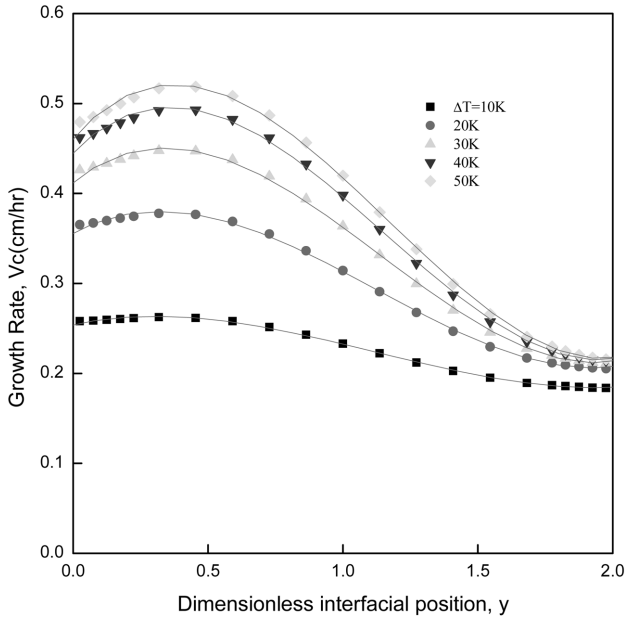


Fig. 10. Interfacial distribution of growth rates along the y-direction of the crystal surface for 10 K $\le \Delta T \le$ 50 K, corresponding to Fig. 2.

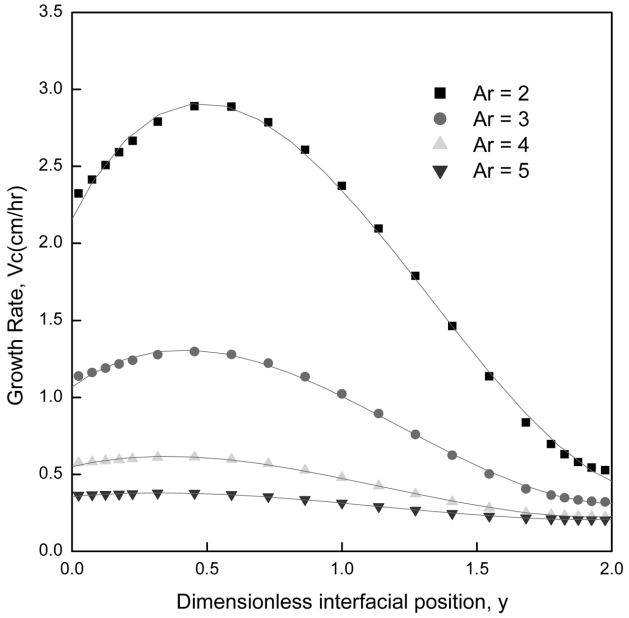


Fig. 11. Interfacial distribution of growth rates along the y-direction of the crystal surface at different aspect ratios of 2, 3, 4, 5, corresponding to Fig. 6.

shows the interfacial distribution of growth rates along the y-direction of the crystal surface at different aspect ratios of 2, 3, 4, 5, corresponding to Fig. 6. Like the different temperature differences, with decreasing the aspect ratio from 5 down to 2, the interfacial distribution of growth rate becomes asymmetrical against y = 1.0 and the maximum growth rate occurs in the neighborhood of y = 0.5. For Ar = 4 and 5, the interfacial distribution of the growth rate exhibits nearly flat, which indicates the diffusion mode is more dominant over the thermo-solutal convection. Fig. 12 shows the interfacial distribution of growth rates along the y-direction of the crystal surface for 10 Torr $\leq P_B \leq$ 200 Torr. With increasing the partial pressure of component B, $P_B$ from 10 to 20 Torr, the interfacial distribution of growth rate becomes asymmetrical against y = 1.0 and the maximum growth rate occurs in the neighborhood of y = 0.5. For 50 Torr $\leq P_B \leq$ 200 Torr, a gap between the maximum growth rates at 50 Torr and 100 Torr in the neighborhood of y = 0.5 becomes enlarged and at 150 Torr and 200 Torr, slightly reduced.

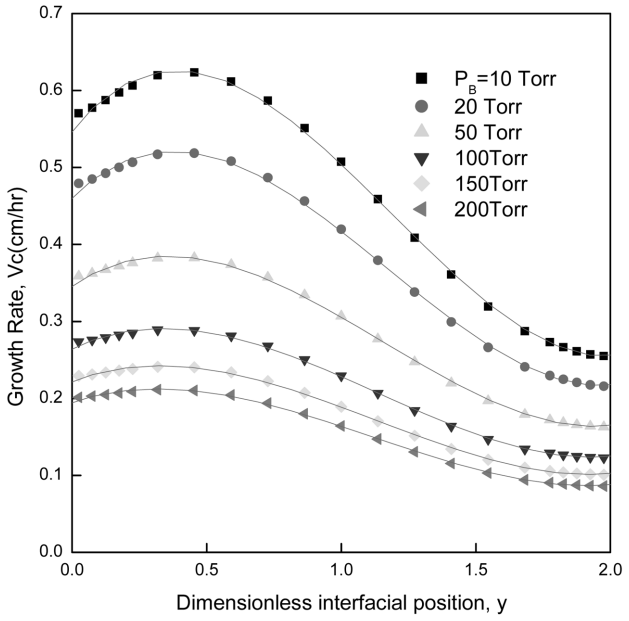


Fig. 12. Interfacial distribution of growth rates along the y-direction of the crystal surface for 10 Torr $\leq P_B \leq$ 200 Torr, corresponding to Fig. 8.

## 4. Conclusions

The parameters under consideration in this study are $\Delta T$ = 50 K, Ar = 5, $P_B$ = 20 Torr, and the corresponding five dimensionless parameters of Pr = 1.18, Le = 0.15, Pe = 2.89, Cv = 1.06, $Gr_t = 3.46 \times 10^4$ and $Gr_s = 6.02 \times 10^5$. It is concluded that for 10 K $\leq \Delta T \leq$ 50 K, the growth rate gradually increases with the temperature difference as a slope of $2.1 \times 10^{-3}$ cm/hr•K. The rate increases with increasing the temperature difference, as a power law of log $\Delta T^n$ with n = 0.224. The rate and the Peclet number and $|U|_{max}$ are directly and intimately dependent on the temperature difference, which indicates thermally buoyancy-driven convection plays an important role in the vapor phase during the physical vapor transport. The rate is second order-exponentially decreased for $2 \leq Ar \leq 5$. This is related to the finding that the effects of side walls tend to stabilize thermo-solutal convection in the growth reactor. In addition, the rate is first order exponentially decayed for $10 \leq P_B \leq 200$ Torr. With increasing the temperature difference from 10 K to 50 K, the interfacial distribution of growth rate becomes asymmetrical against y = 1.0 and the maximum growth rate occurs in the neighborhood of y = 0.5. The same results on the interfacial distribution of growth rates are obtained with decreasing the aspect ratio from 5 down to 2, and with increasing the partial pressure of component B, $P_B$ from 10 Torr up to 200 Torr.

## Acknowledgement

The authors wish to appreciate the financial support provided by the Hannam University through a research

program entitled “Hannam University Hak-sul-yeonku-chosungbi” (starting from April 1, 2010 through March 31, 2011).

## References

[1] N.B. Singh, M. Gottlieb, G.B. Brandt, A.M. Stewart, R. Mazelsky and M.E. Glicksman, “Growth and characterization of mercurous halide crystals:mercurous bromide system,” J. Crystal Growth 137 (1994) 155.
[2] N.B. Singh, R.H. Hopkins, R. Mazelsky and J.J. Conroy, “Purification and growth of mercurous chloride single crystals,” J. Crystal Growth 75 (1970) 173.
[3] S.J. Yosim and S.W. Mayer, “The mercury-mercuric chloride system,” J. Phys. Chem. 60 (1960) 909.
[4] F. Rosenberger, “Fluid dynamics in crystal growth from vapors,” Physico-Chemical Hydro-dynamics 1 (1980).
[5] N.B. Singh, M. Gottlieb, A.P. Goutzoulis, R.H. Hopkins and R. Mazelsky, “Mercurous Bromide acousto-optic devices,” J. Crystal Growth 89 (1988) 527.
[6] B.L. Markham, D.W. Greenwell and F. Rosenberger, “Numerical modeling of diffusive-convective physical vapor transport in cylindrical vertical ampoules,” J. Crystal Growth 51 (1981) 426.
[7] W.M.B. Duval, “Convection in the physical vapor transport process-- I: Thermal,” J. Chemical Vapor Deposition 2 (1994) 188.
[8] A. Nadarajah, F. Rosenberger and J. Alexander, “Effects of buoyancy-driven flow and thermal boundary conditions on physical vapor transport,” J. Crystal Growth 118 (1992) 49.
[9] H. Zhou, A. Zebib, S. Trivedi and W.M.B. Duval, “Physical vapor transport of zinc-telluride by dissociative sublimation,” J. Crystal Growth 167 (1996) 534.
[10] F. Rosenberger, J. Ouazzani, I. Viohl and N. Buchan, “Physical vapor transport revised,” J. Crystal Growth 171 (1997) 270.
[11] G.T. Kim, W.M.B. Duval, N.B. Singh and M.E. Glicksman “Thermal convective effects on physcial vapor transport growth of mercurous chloride crystals ($Hg_2C1_2$) for axisymmetric 2-D cylindrica lenclosure,” Modelling. Simul. Mater. Sci. Eng. 3 (1995) 331.
[12] G.T. Kim, W.M.B. Duval and M.E. Glicksman “Thermal convection in physical vapour transport of mercurous chloride ($Hg_2Cl_2$) for rectangular enclosures,” Modelling. Simul. Mater. Sci. Eng. 5 (1997) 289.
[13] G.T. Kim, W.M.B. Duval and M.E. Glicksman “Effects of asymmetric temperature profiles on thermal convection during physical vapor transport of $Hg_2Cl_2$,” Chem. Eng. Comm. 162 (1997) 45.
[14] J.-G. Choi, K.-H. Lee, M.-H. Kwon and G.-T. Kim, “Effect of accelerational perturbations on physical vapor transport crystal growth under microgravity environments”, J. Korean Crystal Growth and Crystal Technology 16 (2006) 203.
[15] G.-T. Kim and K.-H. Lee, “Parametric studies on convection during the physical vapor transport of mercurous chloride ($Hg_2Cl_2$)”, J. Korean Crystal Growth and Crystal Technology 14 (2004) 281.
[16] G.T. Kim, “Convective-diffusive transport in mercurous chloride ($Hg_2Cl_2$) crystal growth”, J. Ceramic Processing Research 6 (2005) 110.
[17] J.-G. Choi, K.-H. Lee and G.-T. Kim, “Effects of inert gas (Ne) on thermal convection of mercurous chloride system of $Hg_2Cl_2$ and Ne during physical vapor transport, J. Korean Crystal Growth and Crystal Technology 18 (2008) 225.
[18] J.-G. Choi, K.-H. Lee and G.-T. Kim, “Generic studies on thermo-solutal convection of mercurous chloride system of $Hg_2Cl_2$ and Ne during physical vapor transport”, J. Korean Crystal Growth and Crystal Technology 1 (2009) 39.
[19] G.-T. Kim, M.-H. Kwon and K.-H. Lee, “Effects of thermal boundary conditions and microgravity environments on physical vapor transport of $Hg_2Cl_2$-Xe system”, J. Korean Crystal Growth and Crystal Technology 19 (2009) 172.
[20] J.-G. Choi, M.-H. Kwon and G.-T. Kim, “Effects of total pressure and gravity level on the physical vapor transport of $Hg_2Cl_2$-$Cl_2$ system”, J. Korean Crystal Growth and Crystal Technology 19 (2009) 116.
[21] G.-T. Kim and M.H. Kwon, “Theoretical gravity studies on roles of convection in crystal growth of $Hg_2Cl_2$-Xe by physical vapor transport transport under normal and high gravity environments”, J. Korean Crystal Growth and Crystal Technology 19 (2009) 107.
[22] N.B. Singh, R. Mazelsky and M.E. Glicksman, “Evaluation of transport conditions during PVT: mercurous chloride system”, PhysicoChemical Hydrodynamics 11 (1989) 41.
[23] F. Rosenberger and G. Müller, “Interfacial transport in crystal growth, a parameter comparison of convective effects”, J. Crystal Growth 65 (1983) 91.
[24] M. Kassemi and W.M.B. Duval, “Interaction of surface radiation with convection in crystal growth by physical vapor transport”, J. Thermophys. Heat Transfer 4 (1989) 454.
[25] R.B. Bird, W.E. Stewart and E.N. Lightfoot, “Transport Phenomena” (John Wiley and Sons, New York, NY, 1960).
[26] C. Mennetrier and W.M.B. Duval, “Thermal-solutal convection with conduction effects inside a rectangular enclosure”, NASA Technical Memorandum 105371 (1991).
[27] S.V. Patankar, “Numerical Heat Transfer and Fluid Flow” (Hemisphere Publishing Corp., Washington D. C., 1980).
[28] N.B. Singh and W.M.B. Duval, “Growth kinetics of physical vapor transport processes: crystal growth of the optoelectronic material mercurous chloride”, NASA Technical Memorandum 103788 (1991).
[29] C. Mennetrier, W.M.B. Duval and N.B. Singh, “Physical vapor transport of mercurous chloride under a nonlinear thermal profile”, NASA Technical Memorandum 105920 (1992).
[30] I. Catton, “Effect of wall conducting on the stability of a fluid in a rectangular region heated from below”, J. Heat Transfer 94 (1972) 446.